polymers

MDPI

Article

Biocompatible Polymer-Grafted TiO_2 Nanoparticle Sonosensitizers Prepared Using Phosphonic Acid-Functionalized RAFT Agent

Yukiya Kitayama [1,2], Aoi Katayama [2], Zhicheng Shao [1] and Atsushi Harada [1,2,*]

[1] Department of Applied Chemistry, Graduate School of Engineering, Osaka Prefecture University, 1-1 Gakuen-cho, Naka-ku, Sakai 599-8531, Osaka, Japan
[2] Department of Applied Chemistry, Graduate School of Engineering, Osaka Metropolitan University, 1-1 Gakuen-cho, Naka-ku, Sakai 599-8531, Osaka, Japan
* Correspondence: atsushi_harada@omu.ac.jp

Abstract: Sonodynamic therapy is widely used in clinical studies including cancer therapy. The development of sonosensitizers is important for enhancing the generation of reactive oxygen species (ROS) under sonication. Herein, we have developed poly(2-methacryloyloxyethyl phosphorylcholine) (PMPC)-modified TiO_2 nanoparticles as new biocompatible sonosensitizers with high colloidal stability under physiological conditions. To fabricate biocompatible sonosensitizers, a grafting-to approach was adopted with phosphonic-acid-functionalized PMPC, which was prepared by reversible addition–fragmentation chain transfer (RAFT) polymerization of 2-methacryloyloxyethyl phosphorylcholine (MPC) using a newly designed water-soluble RAFT agent possessing a phosphonic acid group. The phosphonic acid group can conjugate with the OH groups on the TiO_2 nanoparticles. We have clarified that the phosphonic acid end group is more crucial for creating colloidally stable PMPC-modified TiO_2 nanoparticles under physiological conditions than carboxylic-acid-functionalized PMPC-modified ones. Furthermore, the enhanced generation of singlet oxygen ($^1O_2$), an ROS, in the presence of PMPC-modified TiO_2 nanoparticles was confirmed using a $^1O_2$-reactive fluorescent probe. We believe that the PMPC-modified TiO_2 nanoparticles prepared herein have potential utility as novel biocompatible sonosensitizers for cancer therapy.

Keywords: sonodynamic therapy; TiO_2; reversible addition–fragmentation chain transfer polymerization; phosphonic acid

Citation: Kitayama, Y.; Katayama, A.; Shao, Z.; Harada, A. Biocompatible Polymer-Grafted TiO_2 Nanoparticle Sonosensitizers Prepared Using Phosphonic Acid-Functionalized RAFT Agent. *Polymers* **2023**, *15*, 2426. https://doi.org/10.3390/polym15112426

Academic Editors: Bruno Henrique Vilsinski, Dina Maria Bairrada Murtinho and Artur J. M. Valente

Received: 27 March 2023
Revised: 15 May 2023
Accepted: 19 May 2023
Published: 23 May 2023

1. Introduction

Ultrasounds with wavelengths beyond human hearing have been widely used in diagnosis and therapy because they can penetrate deep into tissues without radiation damage. Sonodynamic therapy (SDT) has been widely used in clinical studies, including cancer therapy, owing to its non-invasiveness and temporal-spatial controllability with great depth [1–7]. In SDT, reactive oxygen species (ROS) such as singlet oxygen ($^1O_2$) and hydroxyl radicals are generated under ultrasound irradiation, and the ROS induce oxidative damage to target tissues. Furthermore, the generated ROS breaks the redox balance in living cells, which induces effective treatment on the hypoxic tumor [8]. The mechanism of ROS generation is the cavitation effect induced by ultrasounds which causes sonoluminescence, and the phenomenon is attributed to generate ROS from sonosensitizer. For efficient SDTs, sonosensitizers are of great importance to initiate a sonochemical reaction when producing ROS. In the past, many sonosensitizers, such as TiO_2 [9,10], porphyrin and its derivatives [11–14], $BaTiO_3$ [15], and $PtCu_3$ [16,17] have been developed to enhance ROS generation and therapeutic effects. TiO_2 nanoparticles have the potential for targeted delivery to tumors through enhanced permeability and retentivity effects [18,19] owing to their nanometer size [5]. TiO_2 nanoparticles have high chemical and physical stabilities;

however, the colloidal stability of TiO_2 nanoparticles under physiological conditions is poor. TiO_2 nanoparticles have an isoelectric point at pH 6.2 when TiO_2 is formed as an anatase crystal [20]. Thus, TiO_2 nanoparticles have an anionic surface charge at neutral pH and are colloidally stabilized via electrostatic repulsion owing to their anionic charge. However, the electric bilayer on the particles becomes thinner in media containing high ionic concentrations, resulting in poor colloidal stability of the TiO_2 nanoparticles. An important requirement to ensure the efficacy of the sonodynamic therapy is the high colloidal stability of TiO_2 nanoparticles under physiological conditions.

Several approaches have been reported to prepare TiO_2 nanoparticles with high colloidal stability for SDT under physiological conditions. Poly(ethylene glycol) (PEG) modification of TiO_2 nanoparticles is used to create highly stable TiO_2 nanoparticles for various therapies because PEG induces the steric repulsion of the PEG-modified nanoparticles [5,21]. Polysaccharide (e.g., dextran and hyaluronic acid)-modified TiO_2 nanoparticles have also been prepared for sonodynamic cancer therapy [10,22]. In our previous studies, polyion complex (PIC) micelles incorporating TiO_2 nanoparticles were developed as novel sonosensitizers possessing high colloidal stability under physiological conditions [23]. The PIC micelles were prepared from cationic polyallylamine-grafted poly(ethylene glycol) (PAA-*g*-PEG) and anionic TiO_2 nanoparticles at neutral pH, where the micellar structure was stabilized via electrostatic and van der Waals interactions between the polyallylamine and TiO_2 nanoparticles. The PIC micelles possessed high colloidal stability owing to the steric repulsion derived from the PEG grafted on the PIC micelles. Furthermore, we confirmed the sonosensitizing effect of PIC micelles incorporating TiO_2 nanoparticles in vitro with HeLa cells, where decreased cell viability was observed in cells treated with PIC micelles by ultrasound irradiation compared to that in the untreated cells [24].

Recently, reversible deactivation radical polymerization (RDRP) has been developed as an emerging synthetic method to achieve precise molecular design and create various functional polymers via radical reaction [25–44]. Using RDRPs, the surface modification of inorganic nanoparticles can be easily achieved using *grafting-to* or *grafting-from* approaches [45–50]. Charpentier et al. reported the surface-initiated reversible addition–fragmentation chain transfer (RAFT) polymerization of methyl methacrylate from TiO_2 nanoparticles modified with 4-cyano-4-(dodecyl-sulfanylthiocarbonyl) sulfanyl pentanoic acid [51]. Wang et al. reported the successful surface-initiated atom transfer radical polymerization (ATRP) of styrene from TiO_2 nanoparticles using an initiator possessing a trimethoxysilane group [52]. Charpentier et al. reported water-dispersible poly(acrylic acid)-modified TiO_2 nanoparticles by RAFT polymerization from TiO_2 nanoparticles modified with 4-cyano-4-(dodecyl-sulfanylthiocarbonyl)sulfanyl pentanoic acid [53]. Haddleton et al. reported surface modification of 2-(dimethylamino)ethyl methacrylate and 2-(diethylamino)ethyl methacrylate on TiO_2 nanoparticles using *grafting-to* or *grafting-from* approaches with Cu(0)-mediated living radical polymerization using a designed initiator containing catechol as a binding site to TiO_2 [54]. However, to the best of our knowledge, the preparation of biocompatible polymer-modified TiO_2 nanoparticles via RDRPs and their application as sonosensitizers has never been reported.

In this study, we report the fabrication of biocompatible poly(2-methacryloyloxyethyl phosphorylcholine) (PMPC)-modified TiO_2 nanoparticles with high colloidal stability under physiological conditions using RDRPs and investigate the sonosensitizing effect of TiO_2 particles (Scheme 1). To achieve this goal, a RAFT agent containing a phosphonic acid group was newly designed; the phosphonic-acid-functionalized poly(2-methacryloyloxyethyl phosphorylcholine) (PMPC-PO_4H_2) was synthesized via RAFT polymerization with the RAFT agent because the phosphonic acid groups can interact more strongly with the TiO_2 surface compared to carboxylic acids [55–58]. We clarify that the colloidal stability of PMPC-PO_4H_2-modified TiO_2 nanoparticles under physiological conditions was higher than that of poly(2-methacryloyloxyethyl phosphorylcholine) (PMPC) possessing carboxylic acid (PMPC-COOH)-modified TiO_2 nanoparticles; PMPC-COOH was prepared using a commercially available RAFT agent [4-cyano-4-(phenylcarbonothioylthio)pentanoic acid:

RAFT-COOH]. The effect of the molecular weight of PMPC-PO_4H_2 on the colloidal stability of the 2-methacryloyloxyethyl phosphorylcholine (MPC)-modified TiO_2 nanoparticles was also investigated in detail. Finally, the sonosensitizing activity of the PMPC-modified TiO_2 nanoparticles was investigated.

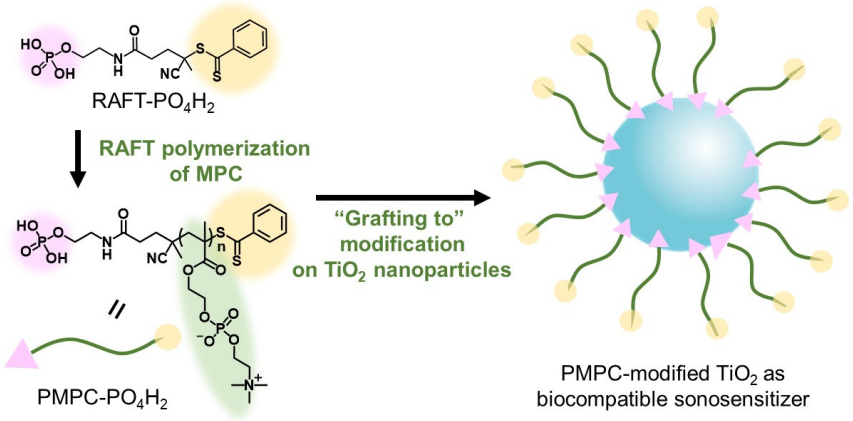

Scheme 1. Schematic of preparation of PMPC-modified TiO_2 nanoparticles as biocompatible sonosensitizer.

2. Results and Discussion

PMPC, developed by Ishihara et al., is water-soluble and has a high biocompatibility derived from the phosphorylcholine motif of the lipid bilayer [59,60]. To modify PMPC as a biocompatible polymer on TiO_2 nanoparticles, a new water-soluble dithiobenzoate-based RAFT agent possessing a phosphonic acid group (RAFT-PO_4H_2) was synthesized, where the phosphonic acid group can form a stable linkage with TiO_2 nanoparticles. 4-Cyano-4-(phenylcarbonothioylthio)pentanoic acid *N*-succinimidyl ester was reacted with *O*-phosphoryl ethanolamine in a mixture of dimethylsulfoxide/water. The product was purified via inverse silica gel chromatography. The purification of the target RAFT agent was confirmed by ^{1}H-NMR and ^{13}C-NMR spectroscopy (see in Figure 1 and Supplementary Materials Figure S1). From ultraviolet-visible (UV–Vis) spectral measurements, RAFT-PO_4H_2 has a maximum absorbance wavelength of 305 nm with a small peak at 480 nm (see in Supplementary Materials Figure S2), indicating that RAFT-PO_4H_2 has a phenylcarbonothioylthio group. RAFT-COOH has a low solubility in water (even under basic conditions); however, RAFT-PO_4H_2 is easily dissolved in water. The high water solubility of RAFT-PO_4H_2 may be attributed to its phosphonic acid and amide groups.

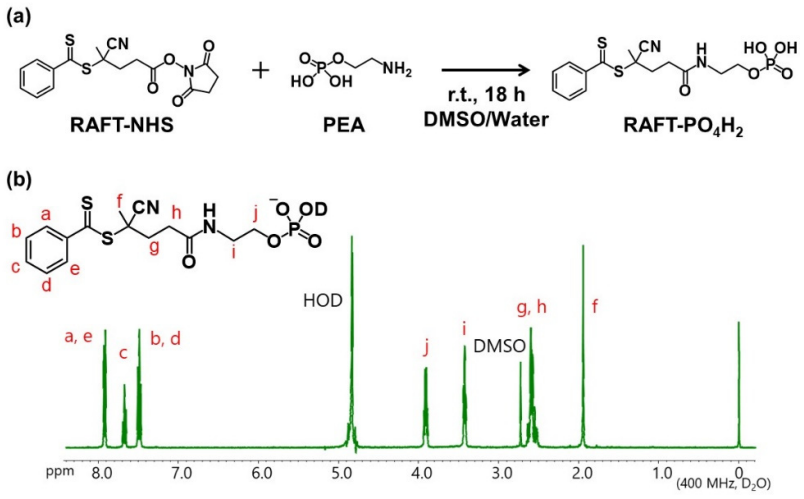

Figure 1. (**a**) Synthetic scheme of RAFT-PO_4H_2. (**b**) ^{1}H NMR spectrum and corresponding chemical structure of RAFT-PO_4H_2.

The polymerization control capability of RAFT-PO_4H_2 as a control agent was investigated via RAFT polymerization of MPC by comparing the performance of RAFT-COOH. In the experiments, the target molecular weights of PMPC were regulated by changing the feed molar ratio of MPC to RAFT-PO_4H_2, where the feed molar ratio [MPC]/[RAFT-PO_4H_2] was set to 10, 20, 40, and 80. Deionized water was selected as the solvent for polymerization. The monomer conversions in all polymerizations using RAFT-PO_4H_2 were estimated to be approximately 99% by ^{1}H-NMR (Figure 2). The number-average molecular weights (M_n) of PMPC prepared using RAFT-PO_4H_2 (PMPC-PO_4H_2) were evaluated to be approximately 5600 (M_w/M_n:1.10), 7600 (M_w/M_n:1.11), 12,000 (M_w/M_n:1.12), and 20,000 (M_w/M_n:1.15) by gel permeation chromatography (GPC) when the target molecular weights were set to 3400, 6300, 12,200, and 24,000, respectively (Table 1). The difference between the experimental and theoretical M_n values was caused by the difference in the excluded volume of the polymer chains between PMPC and PEG, which was used as a standard polymer for preparing a calibration curve for GPC measurements. Methanol was selected as the solvent for RAFT polymerization of MPC with RAFT-COOH because of the low solubility of RAFT-COOH. The conversion of RAFT polymerization of MPC reached 99% at all feed molar ratios of [MPC]/[RAFT-COOH] (see in Supplementary Materials Figure S3). The M_n of PMPC prepared using RAFT-COOH (PMPC-COOH) was evaluated to be approximately 5100 (M_w/M_n:1.11), 6400 (M_w/M_n:1.11), 9800 (M_w/M_n:1.16), and 16,000 (M_w/M_n:1.21) when the target molecular weights were 3200, 6200, 12,100, and 24,000, respectively (Figure 3, Table 1). These results indicate that PMPC-PO_4H_2 and PMPC-COOH were successfully prepared with narrow molecular weight distributions using RAFT-PO_4H_2 and RAFT-COOH, respectively. Furthermore, PMPC-PO_4H_2 and PMPC-COOH showed absorbances at 491 nm and 488 nm, respectively, which were derived from the dithiobenzoate groups of the RAFT end groups (see in Supplementary Materials Figures S4 and S5).

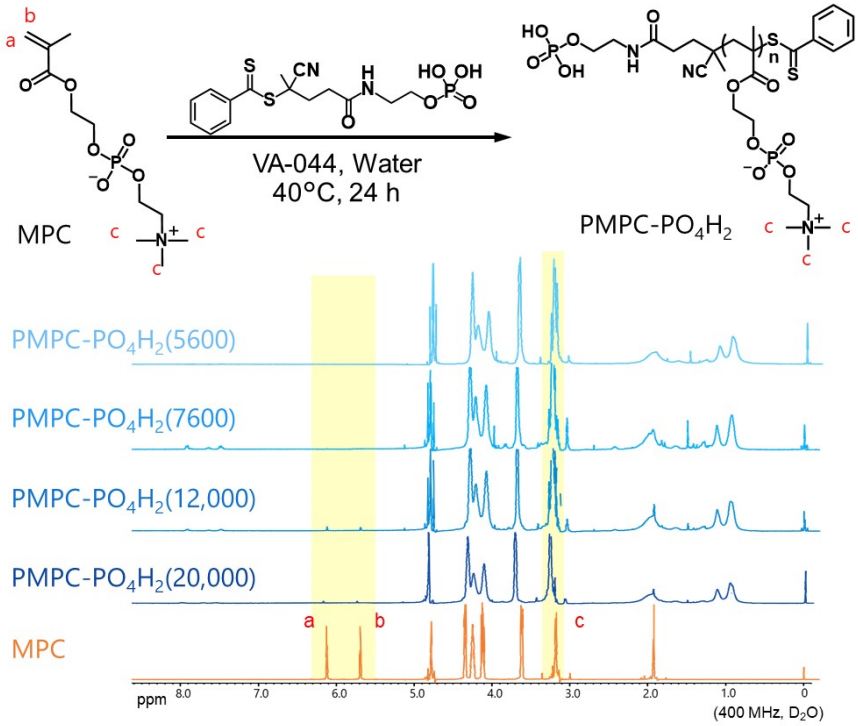

Figure 2. Top: Scheme of RAFT polymerization of MPC with RAFT-PO_4H_2. Bottom: ^{1}H NMR spectra of MPC and polymer solutions obtained after RAFT polymerizations of MPC using RAFT-PO_4H_2 with different molar ratios of MPC and RAFT-PO_4H_2.

Table 1. RAFT polymerization of MPC with RAFT-PO_4H_2 or RAFT-COOH [a].

Run	RAFT Agent	$[MPC]_0/[RAFT\ Agent]_0$/	Conv. (%)	M_n	$M_{n,th}$	M_w/M_n
1 [b]	RAFT-PO_4H_2	10/1	>99	5600	3400	1.10
2 [b]	RAFT-PO_4H_2	20/1	>99	7600	6300	1.11
3 [b]	RAFT-PO_4H_2	40/1	>99	12,000	12,200	1.12
4 [b]	RAFT-PO_4H_2	80/1	>99	20,000	24,000	1.15
5 [c]	RAFT-COOH	10/1	>99	5100	3200	1.11
6 [c]	RAFT-COOH	20/1	>99	6400	6200	1.11
7 [c]	RAFT-COOH	40/1	>99	9800	12,100	1.16
8 [c]	RAFT-COOH	80/1	>99	16,000	24,000	1.21

[a]: Polymerization time: 24 h; Polymerization temperature: 70 °C; Initiator: V-501; [b]: Solvent: deionized water; [c]: Solvent: methanol.

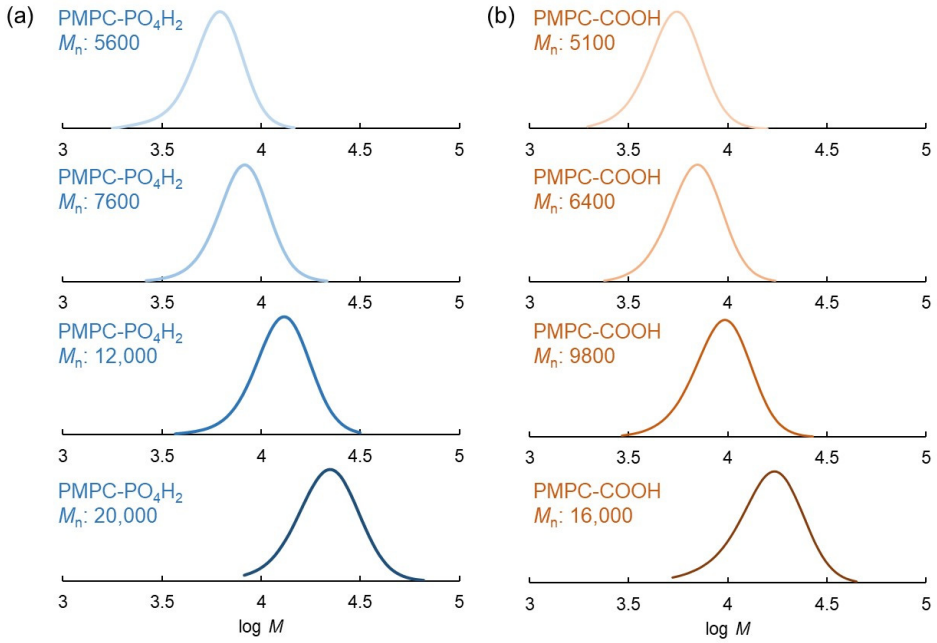

Figure 3. GPC charts of PMPC-PO_4H_2 (**a**) and PMPC-COOH (**b**) obtained after RAFT polymerizations of MPC using RAFT-PO_4H_2 and RAFT-COOH, respectively, with different target molecular weights.

For the preparation of PMPC-modified TiO_2 nanoparticles, we used the *grafting-to* approach to prepare PMPC-modified TiO_2 nanoparticles using PMPC-PO_4H_2 and PMPC-COOH. In the modification step, PMPC-PO_4H_2 was added to the aqueous dispersion of TiO_2 in the presence of polyoxyethylene (20) oleyl ether (Brij98), where the pH of the aqueous media was adjusted to 4.0, to form OH groups on the TiO_2 nanoparticles. Notably, the TiO_2 nanoparticles were coagulated while adjusting to pH 4.0 without Bij98, whereas the particles were stably dispersed upon the addition of Brij98; this phenomenon was caused by the steric repulsion derived from the adsorbed Brij98 on TiO_2 nanoparticles. The adsorption of Brij98 on TiO_2 nanoparticles was supported by zeta potential measurements, that is, the zeta potential of the original TiO_2 nanoparticles (without Brij98) at pH 4.0 was +41.5 mV, whereas the zeta potential of the TiO_2 nanoparticles decreased slightly to +34.6 mV upon addition of Brij98, indicating that Brij98 was slightly adsorbed on the TiO_2 nanoparticles. The Brij98-stabilized TiO_2 nanoparticle dispersion had a monomodal particle size distribution, with a size of 38 nm (PDI: 0.256) (Figure 4). After the modification of PMPC-PO_4H_2 (M_n: 5600) on the TiO_2 nanoparticles, a peak derived from the submicrometer-sized coagulate TiO_2 particles was observed with a peak derived from the non-coagulated TiO_2 particles (average particle size: 55 nm, PDI: 0.256), indicating that the steric repulsion between TiO_2 particles is not effective for maintaining the colloidal stability when using the short PMPC-PO_4H_2. When PMPC-PO_4H_2 of 7600 in M_n was used,

a small coagulate peak was also observed [47.2 nm (PDI: 0.263) for 7600 in M_n]. However, the coagulated TiO_2 particles were not detected when using the other PMPC-PO_4H_2 of 12,000 and 20,000 in M_n [49.3 nm (PDI: 0.194) for 12,000 in M_n, and 55.7 nm (PDI: 0.151) for 20,000 in M_n]. Furthermore, the zeta potential of PMPC-modified TiO_2 nanoparticles prepared with PMPC-PO_4H_2 (M_n: 20,000) decreased markedly to +4.8 mV, which indicates that the modification of PMPC on TiO_2 particles was successful. Moreover, the similar particle size distribution of PMPC-modified TiO_2 particles prepared with PMPC-PO_4H_2 of 12,000, and 20,000 in M_n was maintained even after 240 min in pure water and after 100 times dilution of these particles in pure water [48.2 nm (PDI: 0.203) for 12,000 in M_n, and 53.3 nm (PDI: 0.172) for 20,000 in M_n after 240 min] (see in Supplementary Materials Figure S6). Thus, colloidally stable PMPC-modified TiO_2 nanoparticles were successfully prepared using PMPC-PO_4H_2 with sufficient molecular weight. A similar molecular weight effect on the TiO_2 particle size distribution was observed when using PMPC-COOH with different molecular weights. A notable coagulation of TiO_2 particles was detected in the particle size distribution of TiO_2 particles incubated with PMPC-COOH of 5100 in M_n. However, when PMPC-COOH with a higher molecular weight was used, particle size distributions with small peaks derived from coagulated TiO_2 particles were observed. The zeta potential of PMPC-COOH (M_n: 16,000) was approximately +17.9 mV, which is smaller than that of the original TiO_2 particles but is higher than that of the PMPC-PO_4H_2-modified TiO_2 particles. Furthermore, the average particle size of the PMPC-COOH-modified TiO_2 particles increased [84.0 nm (PDI: 0.236) for 16,000 in M_n, and 102.0 nm (PDI: 0.240) for 9800 in M_n] just after 100 times dilution using pure water; a more marked increase in the particle size of PMPC-COOH-modified TiO_2 particles just after dilution was detected using lower molecular weight PMPC-COOH, although the particle size was maintained after 240 min (see in Supplementary Materials Figure S6). The difference in the colloidal stability of PMPC-PO_4H_2- and PMPC-COOH-modified TiO_2 particles during pure water dilution may be caused by the higher affinity of the PO_4H_2 group to the TiO_2 particles than that of the COOH group. These results indicate that the colloidal stability of PMPC- PO_4H_2-modified TiO_2 particles is higher than that of PMPC-COOH-modified TiO_2 particles against pure water dilution.

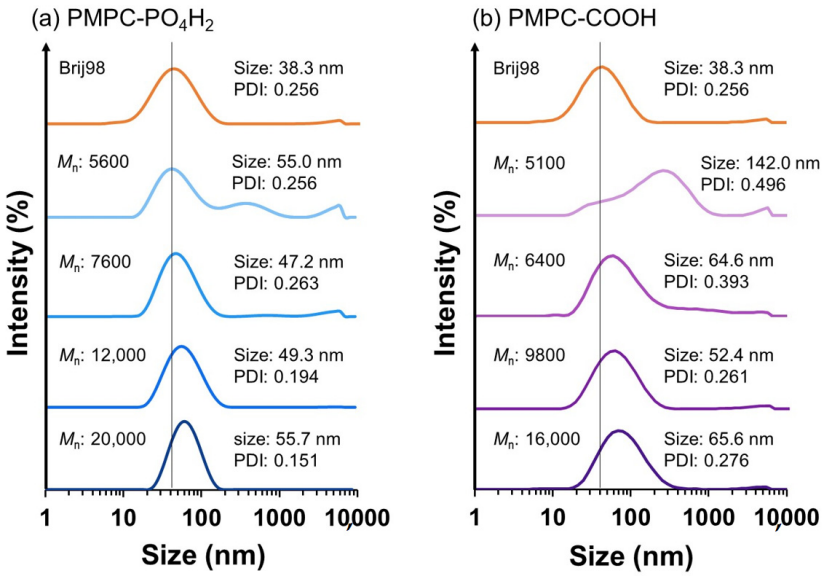

Figure 4. Particle size distributions of PMPC-PO_4H_2- (**a**) and PMPC-COOH- (**b**) modified TiO_2 nanoparticles. PMPC-PO_4H_2 (**a**) and PMPC-COOH (**b**) possessing different molecular weights were obtained after RAFT polymerizations of MPC using RAFT-PO_4H_2 and RAFT-COOH, respectively.

We further investigated the effect of the PMPC-PO_4H_2 concentration on the particle size of obtained PMPC-modified TiO_2 particles using PMPC-PO_4H_2 (M_n: 7600) (see in Supplementary Materials Figure S7 and Table 2). The average particle size of PMPC-

modified TiO_2 particles increased with increasing concentration from 2.5 mg/mL (41.6 nm, PDI: 0.181) to 5.0 mg/mL (49.1 nm, PDI: 0.264). However, the average particle size was almost saturated above 5.0 mg/mL, i.e., 47.2 nm (PDI: 0.263) and 49.3 nm (PDI: 0.271), and a monodispersed distribution was maintained when the PMPC- PO_4H_2 concentration was set to 0, 2.5, 5.0, 10.0, and 20.0 mg/mL, respectively (see in Supplementary Materials Figure S7).

Table 2. Average particle sizes and PDI of TiO_2 nanoparticles before and after modification of PMPC-PO_4H_2. Different concentrations of PMPC-PO_4H_2 were used.

Sample	Concentration (mg/mL)	Size (nm)	PDI
Original	-	38.3	0.256
PMPC-PO_4H_2 [a]	2.5	41.6	0.181
	5.0	49.1	0.264
	10	47.2	0.263
	20	49.3	0.271

[a]: Number-average molecular weight: 7600.

For application as a sonosensitizer, PMPC-modified TiO_2 particles with high colloidal stability under physiological conditions, including pH and ionic concentration, are required. Thus, the colloidal stability of PMPC-modified TiO_2 particles prepared using PMPC-PO_4H_2 and PMPC-COOH was investigated in PBS (pH 7.4) using DLS. The particles of Brij98 stabilized TiO_2 particles immediately coagulated in PBS (Figure 5g). PMPC-modified TiO_2 particles prepared using PMPC-PO_4H_2 (M_n: 5600) showed higher stability than unmodified TiO_2 particles because the particles were not immediately coagulated in PBS. However, the particle size significantly increased with increasing incubation time, reaching 199 nm (PDI: 0.279) after 60 min of incubation. We found that the colloidal stability of the PMPC-modified TiO_2 particles increased with the increasing molecular weight of PMPC-PO_4H_2. The particle sizes of PMPC-modified TiO_2 particles after 60 min of incubation were 86.5 nm (PDI: 0.200), 77.4 nm (PDI: 0.188), and 56.7 nm (PDI: 0.159) when PMPC- PO_4H_2 of 7600, 12,000, and 20,000 in M_n was used, respectively. In particular, the $PMPC_{20,000}$-modified TiO_2 particles were maintained at less than 100 nm even after 240 min of incubation. In contrast to PMPC-PO_4H_2, the particle size of the PMPC-modified TiO_2 nanoparticles increased immediately even when high-molecular-weight PMPC-COOH (9800 and 16,000) was used (Figure 5). These results strongly indicate that the phosphonic acid groups of PMPC-PO_4H_2 are necessary to obtain colloidally stable PMPC-modified TiO_2 nanoparticles under physiological conditions. Previously, to prepare self-assembled monolayers (SAMs) on TiO_2 substrates or to form modification layers of TiO_2 photocatalysts, various molecules possessing acidic functional groups (e.g., carboxylic acid and phosphonic acid) were widely used, where these acidic groups work as interaction sites for the TiO_2 surface [55–58]. Several groups have reported that phosphonic acids interact more strongly with TiO_2 surfaces compared to carboxylic acids [61]. Gao et al. reported that well-ordered SAMs were formed on TiO_2 surfaces with phosphonic acid compounds, whereas most carboxylic acid compounds were removed from the TiO_2 surface during the washing process [62]. Thus, it appears that PMPC-COOH may be desorbed from TiO_2 nanoparticles in the buffered aqueous solution, resulting in particle coagulation, whereas TiO_2 nanoparticles with high colloidal stability were obtained with PMPC- PO_4H_2 and had a stronger interaction capability with TiO_2.

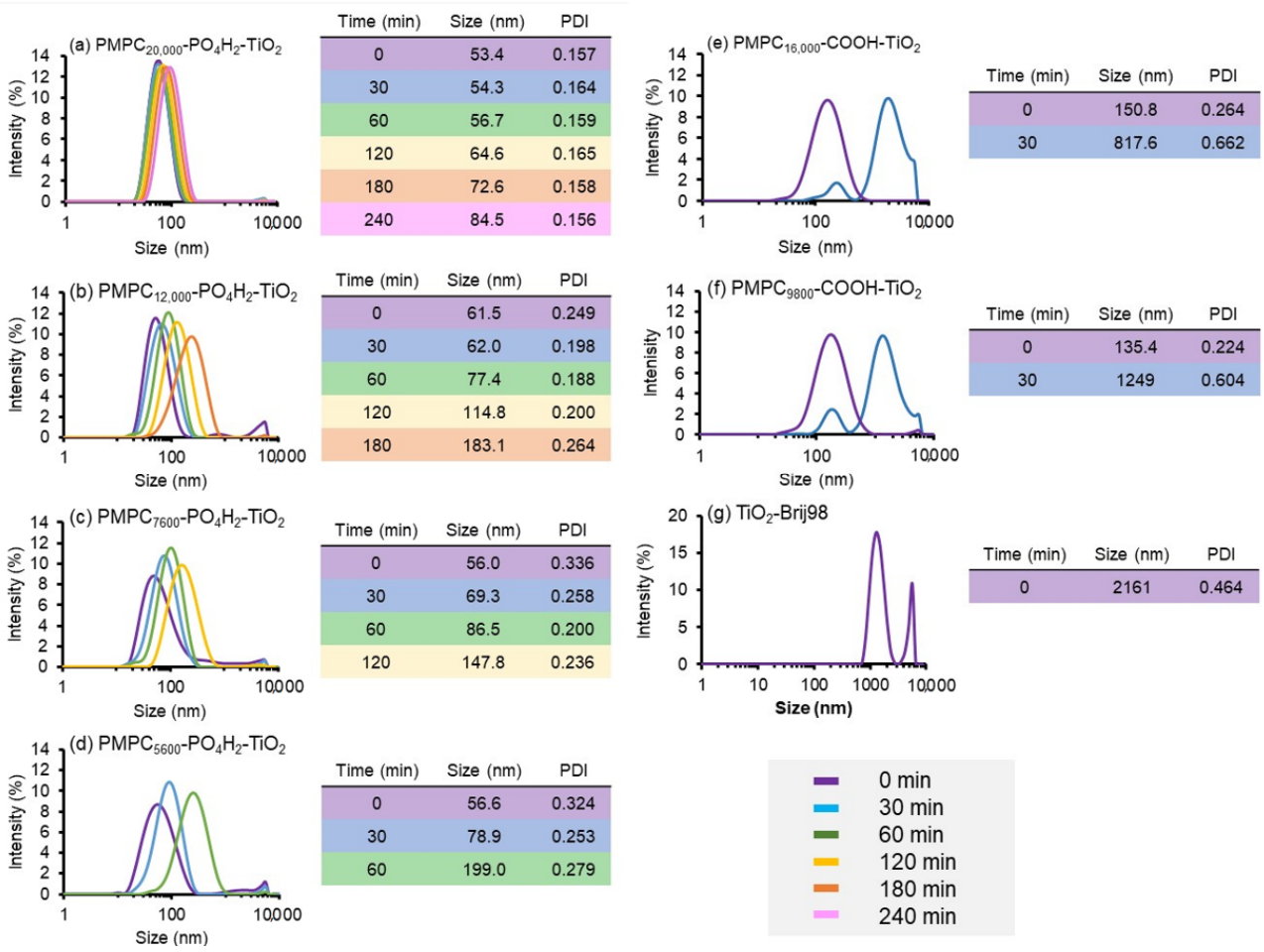

Figure 5. Particle size distributions, average particle size, and PDI values of PMPC-modified TiO_2 nanoparticles prepared with $PMPC_{20,000}$-PO_4H_2 (**a**), $PMPC_{12,000}$-PO_4H_2 (**b**), $PMPC_{7600}$-PO_4H_2 (**c**), $PMPC_{5600}$-PO_4H_2 (**d**), $PMPC_{30,000}$-COOH (**e**), $PMPC_{15,000}$-COOH (**f**), and Brij98-stabilized TiO_2 nanoparticles (**g**) at different incubation times (0 min: purple, 30 min: blue, 60 min: green, 120 min: yellow, 180 min: orange, 240 min: pink) in PBS.

Finally, we investigated the $^1O_2$ generation capability of $PMPC_{20,000}$-PO_4H_2-modified TiO_2 particles under sonication in PBS using singlet oxygen sensor green (SOSG) as a probe molecule; the fluorescence intensity derived from SOSG increases upon reaction with $^1O_2$. As shown in Figure 6, the fluorescence intensity of SOSG increased gradually with increasing sonication time and was significantly higher than that of the control sample in the absence of $PMPC_{20,000}$-PO_4H_2-modified TiO_2 particles (buffer solution). Furthermore, the fluorescence intensity derived from $^1O_2$-reacted SOSG for $PMPC_{20,000}$-PO_4H_2-modified TiO_2 particles was higher than that for $PMPC_{7600}$-PO_4H_2-modified TiO_2 particles. These results indicate that the PMPC-PO_4H_2-modified TiO_2 particles with high colloidal stability in the buffer solution exhibited $^1O_2$ generation ability under sonication conditions in aqueous media.

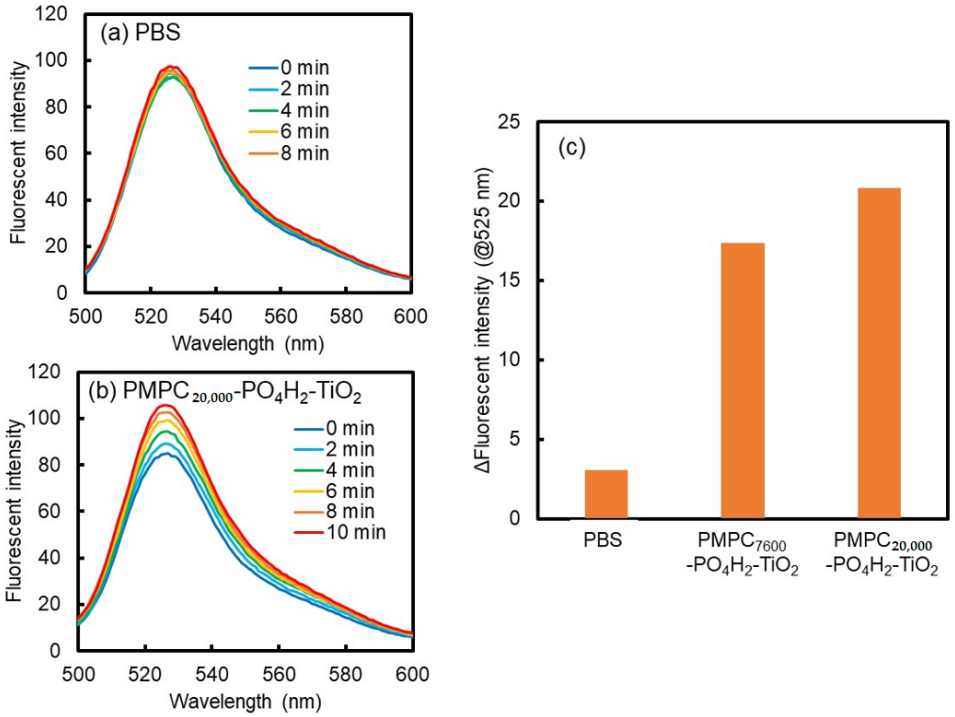

Figure 6. Fluorescence spectra derived from singlet oxygen sensor green at various sonication times in PBS without (**a**) and with $PMPC_{20,000}$-PO_4H_2-modified TiO_2 nanoparticles (**b**). Fluorescent intensity change at 525 nm after 10 min sonication without and with $PMPC_{7600}$-PO_4H_2-modified TiO_2 nanoparticles, and with $PMPC_{20,000}$-PO_4H_2-modified TiO_2 nanoparticles. (**c**) Fluorescent intensity change at 525 nm after 10 min sonication without and with PMPC7600-PO4H2-modified TiO2 nanoparticles, and with PMPC20,000-PO4H2-modified TiO2 nano-particles.

3. Conclusions

In this study, we successfully created PMPC-modified TiO_2 nanoparticles with high colloidal stability in PBS as novel sonosensitizers using PMPC-PO_4H_2. To prepare PMPC-PO_4H_2, a new water-soluble RAFT agent possessing a phosphonic acid group (RAFT-PO_4H_2) was synthesized. Using RAFT-PO_4H_2, PMPC-PO_4H_2 with a narrow molecular weight distribution was prepared. Further, the molecular weight of PMPC-PO_4H_2 could be regulated by changing the molar ratio [MPC]/[RAFT-PO_4H_2]. The *grafting-to* approach using PMPC-PO_4H_2 yielded PMPC-modified TiO_2 nanoparticles, and PMPC-PO_4H_2 with a higher molecular weight yielded greater colloidal stability of the PMPC-modified TiO_2 nanoparticles. Moreover, the PMPC-PO_4H_2-modified TiO_2 nanoparticles had greater colloidal stability under physiological conditions than the PMPC-COOH-modified TiO_2 nanoparticles. Furthermore, the sonosensitizing effect of the PMPC-modified TiO_2 nanoparticles in assisting $^1O_2$ generation in an aqueous medium was clarified. Utilizing the RAFT polymerization, the TiO_2 nanoparticles can be further functionalized. For example, the sonosensitizer can be further functionalized by 2nd block chain extension and/or RAFT chain end modification. We believe that the various functionalized biocompatible polymer-functionalized TiO_2 nanoparticles will be developed for sonodynamic therapy.

4. Materials and Methods

4.1. Materials

4-Cyano-4-(phenylcarbonothioylthio)pentanoic acid *N*-succinimidyl ester, *O*-phosphoryl ethanolamine, and MPC were purchased from Sigma–Aldrich (St. Louis, MO, USA). 2,2′-Azo*bis*[2-(2-imidazolin-2-yl)propane]dihydrochloride (VA-044) and Brij98 were purchased from Wako Pure Chemical Co., Ltd. (Osaka, Japan). NaCl, HCl, NaOH, and dimethyl sulfoxide (DMSO) were purchased from Nacalai Tesque (Kyoto, Japan). A dispersion of

TiO_2 nanoparticles (STS-100) was purchased from Ishihara Sangyo Kaisha Ltd. (Osaka, Japan). Deionized water was obtained using a Millipore Milli-Q purification system. SOSG was purchased from Thermo Fisher Scientific (Waltham, MA, USA).

4.2. Apparatus

UV–Vis spectral measurements were performed using a V-560 spectrophotometer (Jasco Ltd., Tokyo, Japan). Fluorescence spectral measurements were performed using an FP-8300 spectrophotometer (Jasco Ltd., Tokyo, Japan). ^{1}H-NMR spectra were measured using a 400-MHz Fourier transform (FT)-NMR apparatus (JNM-ECX400, FT-NMR system, JEOL Ltd., Tokyo, Japan). The particle size distribution and zeta potential of the obtained particles were measured using a ZETASIZER NANO-ZS instrument (Malvern, UK). Ultrasonication was performed using Sonitron2000 (NEPA GENE, Chiba, Japan). The number- and weight-average molecular weights (M_n and M_w, respectively) were analyzed by GPC at 40 °C using TSKgel G3000PW and TSKgel G4000PW (7.8 mm i.d. × 300 mm, Tosoh Corp.) with 20 mM phosphate buffer (pH 7.4) as the eluent, coupled with a refractive index detector (RI-2031 Plus, JASCO, Tokyo, Japan). A PEG standard (molecular weight range: 1080–107,000) was used to calibrate the molecular weight. Theoretical molecular weights were calculated using the following Equation (1). In Equation (1), $M_{n.Monomer}$ and $M_{n.RAFT}$ are molecular weights of monomer and RAFT agent, respectively, [Monomer] and [RAFT agent] were molar concentrations of monomer and RAFT agent, respectively.

$$M_{n.th} = M_{n.Monomer} \times \frac{[\text{Monomer}]}{[\text{RAFT agent}]} \times \text{Conversion} + M_{n.RAFT} \quad (1)$$

4.3. Synthesis of RAFT- PO_4H_2

4-Cyano-4-(phenylcarbonothioylthio)pentanoic acid *N*-succinimidyl ester (546.6 mg, 1.45 mmol) was dissolved in DMSO (30 mL). *O*-phosphoryl ethanolamine (234.6 mg, 1.66 mmol) was dissolved in a carbonate buffer (pH 9, 15 mL). These solutions were mixed to facilitate a coupling reaction between these molecules at room temperature for 18 h in the dark. The product was purified via inverse silica gel chromatography using methanol and water. Methanol and water were removed by evaporation and freeze-drying, respectively, to yield a dry product. Yield: 82%.

4.4. Synthesis of PMPC by RAFT Polymerization

MPC (1 mmol), RAFT-PO_4H_2 (10, 20, 40, 80 μmol), and VA-044 (2.5, 5.0, 10, 20 μmol) were dissolved in deionized water (3, 3, 5, 8 mL). The solution was added to a Schlenk flask. After several N_2/degassing processes, the polymerization began with heating the solution at 40 °C for 24 h in the dark. After polymerization, the polymer (PMPC-PO_4H_2) was obtained by freeze-drying. To prepare PMPC-COOH, RAFT polymerization was performed under the same conditions as the prepolymer solution of methanol (3 mL) containing MPC (1 mmol), RAFT-COOH (10, 20, 40, and 80 μmol), and VA-044 (2.5, 5.0, 10 and 20 μmol).

4.5. PMPC-Modified TiO_2 Nanoparticles

TiO_2 nanoparticles were dispersed in deionized water by dissolving Brij98 (1.5 mL), and PMPC- PO_4H_2 or PMPC-COOH aqueous solution (1.5 mL) was mixed with the dispersion of TiO_2 nanoparticles (final concentration:1 mg/mL TiO_2, 0.5 mM Brij98, 10 mg/mL PMPC). After the pH was adjusted to 4.0, the mixture was incubated for 24 h at room temperature in the dark. The size distribution of the incubated particles was determined using DLS. The supernatant of the dispersion was separated by ultrafiltration (50,000 Da), and the UV–Vis spectra of the supernatant and the original PMPC aqueous solution were measured to evaluate the modification of PMPC-PO_4H_2 or PMPC-COOH on TiO_2 nanoparticles.

4.6. Colloidal Stability of PMPC-Modified TiO_2 Nanoparticles in PBS

The dispersion of PMPC-modified TiO_2 nanoparticles (2.5 μL) was mixed with PBS (pH 7.4, 2.9975 mL). After several incubation periods, the particle size distributions were measured using DLS. Stabilized TiO_2 nanoparticles were used as a reference instead of PMPC-modified TiO_2 nanoparticles.

4.7. Sonosensitizing Effect of PMPC-Modified TiO_2 Nanoparticles

The dispersion of PMPC-modified TiO_2 nanoparticles (3 mL, TiO_2 concentration: 45 μL/mL) was mixed with a methanol solution of SOSG (0.5 M, 6 μL). Thereafter, sonication (intensity: 0.5 W/cm^2) was performed for 2, 4, 6, 8, and 10 min. The fluorescence intensity of SOSG was measured at excitation wavelength of 485 nm and an emission wavelength of 525 nm.

Supplementary Materials: The following supporting information can be downloaded at: https://www.mdpi.com/article/10.3390/polym15112426/s1, Figure S1: ^{13}C NMR spectrum of RAFT-PO_4H_2; Figure S2: UV–Vis spectrum of RAFT-PO_4H_2; Figure S3: ^1H NMR spectra of MPC and PMPC; Figure S4: UV–Vis spectra of PMPC-PO_4H_2; Figure S5: UV–Vis spectra of PMPC-COOH; Figure S6: Colloidal stability of PMPC-PO_4H_2-and PMPC-COOH-modified TiO_2 particles; Figure S7: Particle size distributions of PMPC-PO_4H_2-modified TiO_2 particles prepared with different concentrations of $PMPC_{7600}$-PO_4H_2.

Author Contributions: Conceptualization, A.H.; methodology, A.H.; investigation, A.K. and Z.S.; writing—original draft preparation, Y.K.; writing—review and editing, A.H.; supervision, A.H.; All authors have read and agreed to the published version of the manuscript.

Funding: This study was supported by JSPS KAKENHI (Grant Number 21H03823).

Institutional Review Board Statement: Not applicable.

Data Availability Statement: The data presented in this study are available in the article.

Acknowledgments: The authors thank Junya Emoto for technical support.

Conflicts of Interest: The authors declare no conflict of interest.

References

1. Qian, X.; Zheng, Y.; Chen, Y. Micro/Nanoparticle-Augmented Sonodynamic Therapy (SDT): Breaking the Depth Shallow of Photoactivation. *Adv. Mater.* **2016**, *28*, 8097–8129. [CrossRef]
2. Son, S.; Kim, J.H.; Wang, X.; Zhang, C.; Yoon, S.A.; Shin, J.; Sharma, A.; Lee, M.H.; Cheng, L.; Wu, J.; et al. Multifunctional sonosensitizers in sonodynamic cancer therapy. *Chem. Soc. Rev.* **2020**, *49*, 3244–3261. [CrossRef] [PubMed]
3. Chen, H.; Zhou, X.; Gao, Y.; Zheng, B.; Tang, F.; Huang, J. Recent progress in development of new sonosensitizers for sonodynamic cancer therapy. *Drug Discov. Today* **2014**, *19*, 502–509. [CrossRef] [PubMed]
4. Tachibana, K.; Feril, L.B., Jr.; Ikeda-Dantsuji, Y. Sonodynamic therapy. *Ultrasonics* **2008**, *48*, 253–259. [CrossRef] [PubMed]
5. Zeng, J.; Gu, C.; Geng, X.; Lin, K.; Xie, Y.; Chen, X. Combined photothermal and sonodynamic therapy using a 2D black phosphorus nanosheets loaded coating for efficient bacterial inhibition and bone-implant integration. *Biomaterials* **2023**, *297*, 122122. [CrossRef]
6. Zhao, Y.; Huang, T.; Wang, S.; Yao, S.; Hu, Q.; Wan, X.; Guo, N.; Zhang, Y.; Li, L. Manganese oxide-modified bismuth oxychloride piezoelectric nanoplatform with multiple enzyme-like activities for cancer sonodynamic therapy. *J. Colloid Interface Sci.* **2023**, *640*, 839–850. [CrossRef]
7. An, J.; He, X.; Ma, H.; Li, Y.; Li, Y.; Zhang, X.; Shuai, Q.; Wang, Y.; Liu, W.; Li, W.; et al. Radionuclide labeled nanocarrier for imaging guided combined radionuclide, sonodynamic, and photothermal therapy of pancreatic tumours. *J. Colloid Interface Sci.* **2023**, *642*, 789–799. [CrossRef]
8. Wei, D.; Yu, Y.; Zhang, X.; Wang, Y.; Chen, H.; Zhao, Y.; Wang, F.; Rong, G.; Wang, W.; Kang, X.; et al. Breaking the Intracellular Redox Balance with Diselenium Nanoparticles for Maximizing Chemotherapy Efficacy on Patient-Derived Xenograft Models. *ACS Nano* **2020**, *14*, 16984–16996. [CrossRef]
9. Han, X.; Huang, J.; Jing, X.; Yang, D.; Lin, H.; Wang, Z.; Li, P.; Chen, Y. Oxygen-Deficient Black Titania for Synergistic/Enhanced Sonodynamic and Photoinduced Cancer Therapy at Near Infrared-II Biowindow. *ACS Nano* **2018**, *12*, 4545–4555. [CrossRef]
10. Gil You, D.; Deepagan, V.G.; Um, W.; Jeon, S.; Son, S.; Chang, H.; Yoon, H.I.; Cho, Y.W.; Swierczewska, M.; Lee, S.; et al. ROS-generating TiO2 nanoparticles for non-invasive sonodynamic therapy of cancer. *Sci. Rep.* **2016**, *6*, 23200. [CrossRef]

11. Huang, P.; Qian, X.; Chen, Y.; Yu, L.; Lin, H.; Wang, L.; Zhu, Y.; Shi, J. Metalloporphyrin-Encapsulated Biodegradable Nanosystems for Highly Efficient Magnetic Resonance Imaging-Guided Sonodynamic Cancer Therapy. *J. Am. Chem. Soc.* **2017**, *139*, 1275–1284. [CrossRef]
12. Zhang, Y.; Yong, L.; Luo, Y.; Ding, X.; Xu, D.; Gao, X.; Yan, S.; Wang, Q.; Luo, J.; Pu, D.; et al. Enhancement of HIFU ablation by sonosensitizer-loading liquid fluorocarbon nanoparticles with pre-targeting in a mouse model. *Sci. Rep.* **2019**, *9*, 6982. [CrossRef]
13. Wang, Z.; Yu, N.; Zhang, J.; Ren, Q.; Li, M.; Chen, Z. Nanoscale Hf-hematoporphyrin frameworks for synergetic sonodynamic/radiation therapy of deep-seated tumors. *J. Colloid Interface Sci.* **2022**, *626*, 803–814. [CrossRef]
14. Lu, Z.; Bai, S.; Jiang, Y.; Wu, S.; Xu, D.; Chen, Y.; Lan, Y.; An, Y.; Mao, J.; Liu, X.; et al. Porphyrin-Based Covalent Organic Framework for Imaging-Guided Cancer Combinatorial Immuno-Sonodynamic Therapy. *Adv. Funct. Mat.* **2022**, *32*, 2207749. [CrossRef]
15. He, D.; Wang, W.; Feng, N.; Zhang, Z.; Zhou, D.; Zhang, J.; Luo, H.; Li, Y.; Chen, X.; Wu, J. Defect-Modified nano-$BaTiO_3$ as a Sonosensitizer for Rapid and High-Efficiency Sonodynamic Sterilization. *ACS Appl. Mater. Int.* **2023**, *15*, 15140–15151. [CrossRef]
16. Zhong, X.; Wang, X.; Cheng, L.; Tang, Y.; Zhan, G.; Gong, F.; Zhang, R.; Hu, J.; Liu, Z.; Yang, X. GSH-Depleted $PtCu_3$ nanocages for chemodynamic- enhanced sonodynamic cancer therapy. *Adv. Funct. Mat.* **2020**, *30*, 1907954. [CrossRef]
17. Cheng, S.; Chen, L.; Gong, F.; Yang, X.; Han, Z.; Wang, Y.; Ge, J.; Gao, X.; Li, Y.; Zhong, X.; et al. PtCu Nanosonosensitizers with Inflammatory Microenvironment Regulation for Enhanced Sonodynamic Bacterial Elimination and Tissue Repair. *Adv. Funct. Mater.* **2023**, *in press*. [CrossRef]
18. Iyer, A.K.; Khaled, G.; Fang, J.; Maeda, H. Exploiting the enhanced permeability and retention effect for tumor targeting. *Drug Discov. Today* **2006**, *11*, 812–818. [CrossRef]
19. Matsumura, Y.; Maeda, H. A new concept for macromolecular therapeutics in cancer chemotherapy: Mechanism of tumoritropic accumulation of proteins and the antitumor agent smancs. *Cancer Res.* **1986**, *46*, 6387–6392.
20. Keller, A.A.; Wang, H.; Zhou, D.; Lenihan, H.S.; Cherr, G.; Cardinale, B.J.; Miller, R.; Ji, Z. Stability and Aggregation of Metal Oxide Nanoparticles in Natural Aqueous Matrices. *Environ. Sci. Technol.* **2010**, *44*, 1962–1967. [CrossRef]
21. Yamaguchi, S.; Kobayashi, H.; Narita, T.; Kanehira, K.; Sonezaki, S.; Kubota, Y.; Terasaka, S.; Iwasaki, Y. Novel Photodynamic Therapy Using Water-dispersed TiO_2-Polyethylene Glycol Compound: Evaluation of Antitumor Effect on Glioma Cells and Spheroids In Vitro. *Photochem. Photobiol.* **2010**, *86*, 964–971. [CrossRef] [PubMed]
22. Shen, S.; Guo, X.; Wu, L.; Wang, M.; Wang, X.; Kong, F.; Shen, H.; Xie, M.; Ge, Y.; Jin, Y. Dual-core@shell-structured Fe3O4-NaYF 4@TiO2 nanocomposites as a magnetic targeting drug carrier for bioimaging and combined chemo-sonodynamic therapy. *J. Mat. Chem. B* **2014**, *2*, 5775–5784. [CrossRef] [PubMed]
23. Harada, A.; Ono, M.; Yuba, E.; Kono, K. Titanium dioxide nanoparticle-entrapped polyion complex micelles generate singlet oxygen in the cells by ultrasound irradiation for sonodynamic therapy. *Biomater. Sci.* **2012**, *1*, 65–73. [CrossRef] [PubMed]
24. Yamamoto, S.; Ono, M.; Yuba, E.; Harada, A. In Vitro Sonodynamic Therapeutic Effect of Polyion Complex Micelles Incorporating Titanium Dioxide Nanoparticles. *Nanomaterials* **2017**, *7*, 268. [CrossRef]
25. Otsu, T. Iniferter concept and living radical polymerization. *J. Polym. Sci. Part A: Polym. Chem.* **2000**, *38*, 2121–2136. [CrossRef]
26. Matyjaszewski, K.; Tsarevsky, N.V. Nanostructured functional materials prepared by atom transfer radical polymerization. *Nat. Chem.* **2009**, *1*, 276–288. [CrossRef]
27. Braunecker, W.A.; Matyjaszewski, K. Controlled/living radical polymerization: Features, developments, and perspectives. *Prog. Polym. Sci.* **2007**, *32*, 93–146. [CrossRef]
28. Hawker, C.J.; Bosman, A.W.; Harth, E. New Polymer Synthesis by Nitroxide Mediated Living Radical Polymerizations. *Chem. Rev.* **2001**, *101*, 3661–3688. [CrossRef]
29. Kamigaito, M.; Ando, T.; Sawamoto, M. Metal-Catalyzed Living Radical Polymerization. *Chem. Rev.* **2001**, *101*, 3689–3745. [CrossRef]
30. Terashima, T. Functional spaces in star and single-chain polymers via living radical polymerization. *Polym. J.* **2014**, *46*, 664–673. [CrossRef]
31. Lutz, J.-F.; Ouchi, M.; Liu, D.R.; Sawamoto, M. Sequence-Controlled Polymers. *Science* **2013**, *341*, 1238149. [CrossRef]
32. Satoh, K. Controlled/living polymerization of renewable vinyl monomers into bio-based polymers. *Polym. J.* **2015**, *47*, 527–536. [CrossRef]
33. Yamago, S. Precision Polymer Synthesis by Degenerative Transfer Controlled/Living Radical Polymerization Using Organotellurium, Organostibine, and Organobismuthine Chain-Transfer Agents. *Chem. Rev.* **2009**, *109*, 5051–5068. [CrossRef]
34. Goto, A.; Fukuda, T. Kinetics of living radical polymerization. *Prog. Polym. Sci.* **2004**, *29*, 329–385. [CrossRef]
35. Goto, A.; Zushi, H.; Hirai, N.; Wakada, T.; Tsujii, Y.; Fukuda, T. Living radical polymerizations with germanium, tin, and phosphorus catalysts—Reversible chain transfer catalyzed polymerizations (RTCPs). *J. Am. Chem. Soc.* **2007**, *129*, 13347–13354. [CrossRef]
36. Goto, A.; Suzuki, T.; Ohfuji, H.; Tanishima, M.; Fukuda, T.; Tsujii, Y.; Kaji, H. Reversible Complexation Mediated Living Radical Polymerization (RCMP) Using Organic Catalysts. *Macromolecules* **2011**, *44*, 8709–8715. [CrossRef]
37. Rosen, B.M.; Percec, V. Single-Electron Transfer and Single-Electron Transfer Degenerative Chain Transfer Living Radical Polymerization. *Chem. Rev.* **2009**, *109*, 5069–5119. [CrossRef]
38. Moad, G.; Rizzardo, E.; Thang, S. Living radical polymerization by the raft process—A second update Aust. *J. Chem.* **2009**, *62*, 1402–1472.

39. Corrigan, N.; Jung, K.; Moad, G.; Hawker, C.J.; Matyjaszewski, K.; Boyer, C. Reversible-deactivation radical polymerization (Controlled/living radical polymerization): From discovery to materials design and applications. *Prog. Polym. Sci.* **2020**, *111*, 101311. [CrossRef]
40. David, G.; Boyer, C.; Tonnar, J.; Ameduri, B.; Lacroix-Desmazes, P.; Boutevin, B. Use of Iodocompounds in Radical Polymerization. *Chem. Rev.* **2006**, *106*, 3936–3962. [CrossRef]
41. Kitayama, Y.; Okubo, M. Emulsifier-free, organotellurium-mediated living radical emulsion polymerization (emulsion TERP) of styrene: Poly(dimethylaminoethyl methacrylate) macro-TERP agent. *Polym. Chem.* **2013**, *5*, 2784–2792. [CrossRef]
42. Kitayama, Y.; Chaiyasat, A.; Minami, H.; Okubo, M. Emulsifier-Free, Organotellurium-Mediated Living Radical Emulsion Polymerization of Styrene: Polymerization Loci. *Macromolecules* **2010**, *43*, 7465–7471. [CrossRef]
43. Zetterlund, P.B.; Kagawa, Y.; Okubo, M. Controlled/Living Radical Polymerization in Dispersed Systems. *Chem. Rev.* **2008**, *108*, 3747–3794. [CrossRef] [PubMed]
44. Zetterlund, P.B.; Thickett, S.C.; Perrier, S.; Bourgeat-Lami, E.; Lansalot, M. Controlled/Living Radical Polymerization in Dispersed Systems: An Update. *Chem. Rev.* **2015**, *115*, 9745–9800. [CrossRef] [PubMed]
45. Wang, B.; Li, B.; Zhao, B.; Li, C. Amphiphilic Janus gold nanoparticles via combining "solid-state grafting-to" and "grafting-from" methods. *J. Am. Chem. Soc.* **2008**, *130*, 11594–11595. [CrossRef]
46. Wang, Y.-X.; Li, Y.; Qiao, S.-H.; Kang, J.; Shen, Z.-L.; Zhang, N.-N.; An, Z.; Wang, X.; Liu, K. Polymers via Reversible Addition–Fragmentation Chain Transfer Polymerization with High Thiol End-Group Fidelity for Effective Grafting-To Gold Nanoparticles. *J. Phys. Chem. Lett.* **2021**, *12*, 4713–4721. [CrossRef]
47. Biggs, C.; Walker, M.; Gibson, M. "Grafting to" of RAFTed responsive polymers to glass substrates by thiol-ene and critical comparison to thiol-gold coupling. *Biomacromolecules* **2016**, *17*, 2626–2633. [CrossRef]
48. Li, D.; He, Q.; Li, J. Smart core/shell nanocomposites: Intelligent polymers modified gold nanoparticles. *Adv. Colloid Interface Sci.* **2009**, *149*, 28–38. [CrossRef]
49. Kitayama, Y.; Takeuchi, T. Localized Surface Plasmon Resonance Nanosensing of C-Reactive Protein with Poly(2-methacryloyloxyethyl phosphorylcholine)-Grafted Gold Nanoparticles Prepared by Surface-Initiated Atom Transfer Radical Polymerization. *Anal. Chem.* **2014**, *86*, 5587–5594. [CrossRef]
50. Kitayama, Y.; Takeuchi, T. Synthesis of CO_2/N_2-triggered reversible stability-controllable poly(2-(diethylamino)ethyl methacrylate)-grafted-AuNPs by surface-initiated atom transfer radical polymerization. *Langmuir* **2014**, *30*, 12684–12689. [CrossRef]
51. Hojjati, B.; Charpentier, P. Synthesis and kinetics of graft polymerization of methyl methacrylate from the RAFT coordinated surface of nano-TiO_2. *J. Polym. Sci. A Polym. Chem.* **2008**, *46*, 3926–3937. [CrossRef]
52. Wang, W.; Cao, H.; Zhu, G.; Wang, P. A facile strategy to modify TiO_2 nanoparticles via surface-initiated atrp of styrene. *J. Polym. Sci. A Polym. Chem.* **2010**, *48*, 1782–1790. [CrossRef]
53. Hojjati, B.; Sui, R.; Charpentier, P. Synthesis of TiO_2/PAA nanocomposite by RAFT polymerization. *Polymer* **2007**, *48*, 5850–5858. [CrossRef]
54. Guo, S.; Zhang, Q.; Wang, D.; Wang, L.; Lin, F.; Wilson, P.; Haddleton, D. Bioinspired coating of TiO_2 nanoparticles with antimicrobial polymers by Cu(0)-LRP: Grafting to vs. grafting from. *Polym. Chem.* **2017**, *8*, 6570–6580. [CrossRef]
55. Gao, W.; Dickinson, L.; Grozinger, C.; Morin, F.; Reven, L. Order-disorder transitions in self-assembled monolayers: A 13C solid-state NMR study. *Langmuir* **1997**, *13*, 115–118. [CrossRef]
56. Pawsey, S.; Yach, K.; Halla, J.; Reven, L. Self-Assembled Monolayers of Alkanoic Acids: A Solid-State NMR Study. *Langmuir* **2000**, *16*, 3294–3303. [CrossRef]
57. Zhao, D.; Chen, C.; Wang, Y.; Ji, H.; Ma, W.; Zang, L.; Zhao, J. Surface Modification of TiO_2 by Phosphate: Effect on Photocatalytic Activity and Mechanism Implication. *J. Phys. Chem. C* **2008**, *112*, 5993–6001. [CrossRef]
58. Yu, J.C.; Ho, W.; Yu, J.; Hark, S.K.; Iu, K. Effects of Trifluoroacetic Acid Modification on the Surface Microstructures and Photocatalytic Activity of Mesoporous TiO_2 Thin Films. *Langmuir* **2003**, *19*, 3889–3896. [CrossRef]
59. Ishihara, K.; Ziats, N.P.; Tierney, B.P.; Nakabayashi, N.; Anderson, J.M. Protein adsorption from human plasma is reduced on phospholipid polymers. *J. Biomed. Mater. Res.* **1991**, *25*, 1397–1407. [CrossRef]
60. Ishihara, K.; Nomura, H.; Mihara, T.; Kurita, K.; Iwasaki, Y.; Nakabayashi, N. Why do phospholipid polymers reduce protein adsorption? *J. Biomed. Mater. Res.* **1998**, *39*, 323–330. [CrossRef]
61. Pawsey, S.; Yach, K.; Reven, L. Self-Assembly of Carboxyalkylphosphonic Acids on Metal Oxide Powders. *Langmuir* **2002**, *18*, 5205–5212. [CrossRef]
62. Gao, W.; Dickinson, L.; Grozinger, C.; Morin, F.G.; Reven, L. Self-Assembled Monolayers of Alkylphosphonic Acids on Metal Oxides. *Langmuir* **1996**, *12*, 6429–6435. [CrossRef]